Radiation environment investigations during ExoMars missions to Mars – Objectives, experiments and instrumentation

Article *in* Comptes rendus de l'Académie bulgare des sciences: sciences mathématiques et naturelles · January 2015

CITATIONS
0

READS
99

21 authors, including:

Jordanka Semkova
Bulgarian Academy of Sciences
53 PUBLICATIONS **306** CITATIONS
SEE PROFILE

Tsvetan Dachev
Bulgarian Academy of Sciences
173 PUBLICATIONS **1,190** CITATIONS
SEE PROFILE

V.V. Benghin
Институт медико-биологических пр...
67 PUBLICATIONS **401** CITATIONS
SEE PROFILE

Vyacheslav Shurshakov
Институт медико-биологических пр...
163 PUBLICATIONS **983** CITATIONS
SEE PROFILE

Доклади на Българската академия на науките
Comptes rendus de l'Académie bulgare des Sciences
Tome 68, No 4, 2015

SCIENCES COSMIQUES

Système solaire

RADIATION ENVIRONMENT INVESTIGATIONS DURING EXOMARS MISSIONS TO MARS – OBJECTIVES, EXPERIMENTS AND INSTRUMENTATION

J. Semkova, T. Dachev, St. Maltchev, B. Tomov, Yu. Matviichuk, P. Dimitrov, R. Koleva, I. Mitrofanov*, A. Malakhov*, M. Mokrousov*, A. Sanin*, M. Litvak*, A. Kozyrev*, V. Tretyakov*, D. Golovin*, S. Nikiforov*, A. Vostrukhin*, F. Fedosov*, N. Grebennikova*, V. Benghin, V. Shurshakov****

(*Submitted by Corresponding Member P. Velinov on March 21, 2015*)

Abstract

Deep space manned missions are already a near future of astronautics. Radiation risk on such a long-duration journey appears to be one of the basic factors in planning and designing the mission. The paper relates to the scientific objectives and experiments for investigation of the radiation environment to be carried out during the ExoMars 2016 and 2018 joint missions of the European Space Agency (ESA) and the Federal Space Agency of Russia (Roscosmos) to Mars. The following topics are described: 1) The charged particle telescope and the experiment Liulin-MO for measuring the radiation environment on board the ExoMars 2016 Trace Gas Orbiter satellite as a part of the Fine Resolution Epithermal Neutron Detector (FREND) and 2) Liulin-ML experiment and instrument for investigating the radiation environment on Mars as a part of the active detector of neutrons and gamma rays (ADRON) on the Russian surface platform for ExoMars 2018 mission. Liulin detectors will be used in combination with the neutron detectors to study the radiation conditions both from charged particles and neutrons during the cruise phase, in Mars orbit and on the surface of Mars.

Key words: space radiation, radiation risk, space radiation measurements, interplanetary missions, ExoMars

This work is partly supported by Contracts 503/2-13 and 63/4-14 between SRTI, Bulgarian Academy of Sciences, and SRI, Russian Academy of Sciences.

1. Introduction. The deep space manned missions are already a near future of astronautics. Radiation risk on such a long-duration journey, a great part of which will take place in the interplanetary space, appears to be one of the basic factors in planning and designing the mission.

The estimation of the radiation effects for a long-duration manned space mission requires three distinct procedures: i) Knowledge and modelling of the particle radiation environment; ii) Calculation of primary and secondary particle transport through shielding materials; and iii) Assessment of the biological effect of the dose.

1.1. Sources of ionizing radiation in the interplanetary space. The radiation field in interplanetary space is complex, composed of galactic cosmic rays (GCR), solar energetic particles (SEP), and secondary radiation produced in the shielding materials of the spacecraft and in the biological objects.

The GCR-charged particles that originate from sources beyond the Solar System are the dominant radiation component in the interplanetary radiation environment. GCR represent a continuous radiation source and they are the most penetrating among the major types of ionizing radiation [1]. The distribution of GCR is believed to be isotropic throughout the interstellar and interplanetary space. The energies of GCR particles can reach 10^{20} eV/nucleon. Most of the deleterious effects with regard to health produced by this radiation are associated with nuclei in the energy range from several hundred MeV/nucleon to a few GeV/nucleon. The flux and spectra of those particles show modulation that anti-correlate with the solar activity. The GCR spectrum consists of 98% protons and heavier ions (baryon component) and 2% electrons and positrons (lepton component). The baryon component is composed of 87% protons, 12% helium ions (alpha particles) and 1% heavy ions [2]. The highly energetic particles in the heavy ion component, typically referred to as high Z and energy (HZE) particles, play a particularly important role in space dosimetry [3] and affect strongly the biological objects and humans in space [4]. HZE particles, especially iron, possess high linear energy transfer (LET) and are highly penetrating, which gives them a large potential for radiobiological damage [5]. The average dose rate from GCR in the interplanetary space measured by the RADOM instrument on the Chandrayaan-1 satellite [6] during low solar activity was 12–13 μGy h^{-1}.

Solar energetic particles (SEP) are randomly distributed events, but they may deliver very high doses over short periods and that is why they could be associated with the lethal equivalent doses. The SEP are mainly produced by solar flares, sudden sporadic eruptions of the Sun chromosphere. High fluxes of charged particles (mostly protons, some helium and heavier ions) with energies up to several GeV and intensity up to 10^4 particle cm^{-2} s^{-1} sr^{-1} are emitted. The time profile of a typical SEP event starts with a rapid increase in flux, reaching a peak in minutes to hours. Although SEPs are more likely to occur around solar maximum, such events are at present unpredictable with regard to their

times of occurrence and it cannot be assumed that SEPs will not occur under solar minimum. The most intense solar proton fluencies observed were those in August 1972 and October 1989. The flare containing the largest peak flux of highly penetrating particles was in February 1956 [7–10]. On this basis the so-called worst-case flare is composed, which is thought to occur once a century, but statistics are extremely poor.

1.2. Radiation environment on Mars. The radiation environment on the surface of Mars is much harsher than that on the surface of the Earth for two reasons: Mars lacks a global magnetic field to deflect energetic GCR and SEP, and the Martian atmosphere is much thinner ($< 1\%$) than that of Earth, providing little shielding against the high-energy particles that are incident at the top of its atmosphere. Both GCRs and SEPs interact with the atmosphere and, if energetic enough, penetrate into the Martian soil, or regolith, where they produce secondary particles (including neutrons and γ-rays) that contribute to the complex radiation environment on the Martian surface.

The cosmic rays produce ionization in the ionosphere, atmosphere, hydrosphere, cryosphere and lithosphere of the planets [7–10]. The contribution of cosmic rays to ionization of the outer planetary ionospheres and atmospheres increases with the increment of the planetary distances from the Sun.

2. Implications for future human missions to Mars. The currently adopted NASA ionizing radiation exposure limits allow for astronauts a maximum annual dose of 0.5 Sv to the blood-forming organs (BFO) [11]. The Russian standards for manned space missions allow also 0.5 Sv a year, but not more than 1 Sv for the cosmonaut's career [12]. The recommended ESA and Canadian astronaut's career dose limit is also 1 Sv.

To prepare future human exploration of Mars transport models developed in ([13–17] and references therein) are used for prediction of the particle flux, absorbed dose, dose equivalent and ionization by GCR and SEPs.

Model estimations show that (see [18]): i) behind relatively thin shielding the annual dose equivalent to the BFO from GCR is larger than the annual limit of 0.5 Sv/year; ii) the dose equivalent is a slowly decreasing function of the shield thickness. As it is pointed out in [18] the uncertainties and the possible inaccuracies involved in the calculations could result in a potential shield mass increase by up to a factor of 4. If the exposure is underestimated by a factor of 2, then the shield mass must be increased by an order of magnitude.

Model calculations [19] give a dose rate of about 0.42 Sv h^{-1} to the unshielded BFO for a standard solar proton event and up to 0.70 Sv h^{-1} for the worst-case solar proton event. Under these estimations the necessity of effective shielding is more than evident. Shielding against solar energetic particles is, at first glance, simpler than against GCR. However the benefit of less penetration of the flare particles because of their softer spectrum is offset to a large degree by their high intensity. In addition, solar energetic particles also produce secondaries, which

build up in the shielding materials. In particular the commonly used aluminum proves to be an insufficiently effective shielding material [7–10].

GCR and SEP events affect the evolution of the climate of Mars, the operation of satellites, and the human exploration of the planet. They can affect the chemistry on the surface. The energetic inputs also have an impact on the planetary atmosphere evolution by modifying the escape rates and the chemistry of the upper atmosphere (see [17] and references therein). The determination of the Martian surface and sub-surface radiation environment is an ongoing effort that started with numerical simulations [20, 21].

Present calculations with the available models show that radiation doses expected on manned missions to Mars can easily exceed the suggested allowed doses [16], but we must keep in mind that these estimations bear a lot of uncertainties. Validation of the radiation model predictions available must be secured before any human mission to Mars is undertaken [22]. Therefore experimental measurements of radiation environment characteristics on unmanned missions like ExoMars are of a great importance for the future planning of manned mission in the interplanetary space and on the surface of Mars.

The most recent investigations during the sojourn to Mars and on Mars surface performed aboard of NASA Mars Science Laboratory (MSL, Curiosity) by RAD instrument estimate a total mission dose equivalent of ~ 1.01 Sv for a round trip Mars surface mission with 180 days (each way) cruise, and 500 days on the Martian surface for the 2012–2013 weak solar maximum [23, 24]. The bigger part of that dose (662 ± 108 mSv), which approaches two-thirds of the career exposure limit recognized at NASA to carry a 3% increased risk of fatal cancer at the upper 95% confidence level, would be accumulated during the cruise phase. That dose is also two-thirds of the career exposure limit recognized at Russia, ESA and Canada. It was noted that only about 5.4% of the contribution to the estimated total dose equivalent from both GCR and SEP events of 466 ± 84 mSv during the 253 days MSL's cruise to Mars was due to SEPs and it was surmised (given the relatively low activity profile of solar cycle 24) that the SEP contribution could have been many times larger had it been measured in a different time frame.

Since 1989 the Liulin type dosemeters-spectrometers have been conducting measurements of the radiation environment characteristics on board a number of manned and unmanned spacecrafts in low Earth orbits or in the interplanetary space [25]. New Liulin type instrumentation will be used for radiation investigations during the upcoming ExoMars missions to Mars.

3. ExoMars mission. ExoMars is a joint investigation of Mars to be carried out by ESA and Roscosmos that has two launches foreseen, in 2016 and 2018. Establishing if life ever existed on Mars is one of the outstanding scientific questions of our time. To address this important goal the ExoMars programme has been established to investigate the Martian environment and to demonstrate new technologies paving the way for a future Mars sample return mission in

the 2020's (http://exploration.esa.int/mars/46048-programme-overview). Planned for launch in 2016, its first element, the Trace Gas Orbiter (TGO) satellite, will spend at least one Martian year orbiting the planet.

Two dosemeters and dosemetric experiments are envisaged for the ExoMars mission. The first one is the charged particle telescope and the experiment Liulin-MO for measurement the radiation environment on board the ExoMars 2016 TGO. Liulin-MO is a part of the Fine Resolution Epithermal Neutron Detector (FREND) on TGO. FREND instrument will measure thermal, epithermal and high energy neutrons with energies ranging up to 10 MeV, whose variations are an excellent signature of H bearing substances presence in the Mars regolith at up to 1 m depth (http://l503.iki.rssi.ru/FREND-en.html). The FREND's dosemeter module Liulin-MO is another important part of the system providing information for the radiation environment during the cruise stage and in Mars' orbit. The second envisaged experiment is the Liulin-ML experiment for investigation of the radiation environment on Mars surface. The experiment will be conducted with the Liulin-ML dosemeter as a part of the active detector of neutrons and gamma rays (ADRON) on the Russian surface platform for ExoMars 2018 mission.

4. Liulin-MO and Liulin-ML scientific objectives. The main goal of the Liulin-MO and Liulin-MO dosemetric experiments is investigation of the radiation conditions in the heliosphere at distances from 1 to 1.5 AU from the Sun and on Mars. More detailed objectives are to provide during the cruise phase, in Mars orbit and on Mars surface:

- Measurements of the energy deposition spectra, dose rate and particle flux that allow calculation of the absorbed dose D. Measurements of the LET spectra in silicon, that allow assessment of LET in water LET(H_2O) and then calculation of the radiation quality factor Q according to the $Q(L)$ relationship given in ICRP-60 [26], where L stays for LET:

$$Q = \int Q(L)D(L)\,dL/D. \tag{1}$$

  $Q(L)$ is related functionally to the unrestricted LET or LET(H_2O) of a given radiation. The quality factor (Q) describes the different biological effectiveness of the various radiation types. The biologically significant dose equivalent H is obtained as the absorbed dose is weighted by the corresponding quality factor $H = D \times Q$.

- Estimate the contribution of electrons, protons, heavier ions of GCR and SEP as well as of secondary charged particles and γ radiation in the absorbed dose and the dose equivalent composition.

- Investigate the journal and seasonal variations of the radiation characteristics on Mars' surface.

The data from Liulin-MO on TGO and Liulin-ML on the ExoMars 2018 surface platform will allow comparison of the orbital and surface Mars radiation conditions.

The combined data from the dosemeters and neutron detectors of FREND and ADRON will allow assessment of both the charged particle and the neutron fluxes and doses over broad energy ranges during periods of quiet Sun and during SEP events.

Data obtained will serve for verification and benchmarking of the radiation environment models and assessment of the radiation risk to the crew members of future exploratory flights.

An additional goal of the Liulin-MO and Liulin-ML experiments is to increase the accuracy of the neutron measurements by providing information about radiation fluctuations from charged particles that can have an impact on the signals from the neutron detectors of the FREND and ADRON instruments.

5. Liulin-MO and Liulin-ML description. The Liulin-MO flight and spare models have been developed and space flight qualified. Liulin-MO is a further development of the Liulin-5 and Liulin-Phobos particle telescopes already flown in space [25, 27–30]. The Liulin-MO particle telescope contains two dosemetric telescopes – D1&D2, and D3&D4 arranged at two perpendicular directions. The functional diagram of the instrument is shown in Fig. 1. Every pair of the dosemetric telescopes consists of two 300 μm thick, 20×10 mm area Si PIN photodiodes. The detectors D1 to D4, the charge-sensitive preamplifiers – shaping amplifiers CSA1 to CSA4, the threshold discriminators and the voltage bias circuits are mounted in a separate detector's volume inside the box of the Liulin-MO instrument and are connected to printed circuit boards that contain pulse height

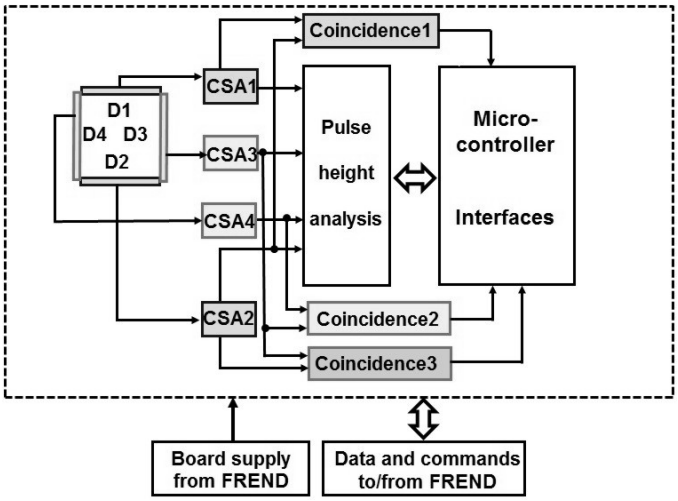

Fig. 1. Functional diagram of Liulin-MO particle telescope

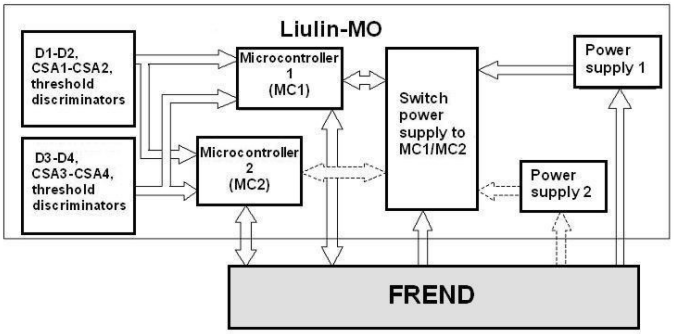

Fig. 2. Block diagram of Liulin-MO

analysis circuits, DC-DC converters, microcontrolers, and interfaces to FREND. The entire package Liulin-MO has a mass of 0.7 kg and consumes 2.2 W. All major units of Liulin-MO are duplicated in order to increase the reliability of the dosemeter. The block diagram is shown in Fig. 2. All detectors D1 to D4 and their electronics, one microcontroler MC1 or MC2 and one power supply unit operate at every moment. The picture of the FREND accommodation on the TGO (Credit: Thales Alenia Space – France `http://exploration.esa.int/mars/48523-trace-gas-orbiter-instruments/?fbodylongid=2217`) is shown in Fig. 3*A*. FREND instrument with mounted on it Liulin-MO is shown in Fig. 3*B*. The external view of Liulin-MO is shown in Fig. 3*C*.

The main measured parameters are the amplitudes of the voltage pulses at the CSA1–CSA4 outputs (see Fig. 1). The amplitude of a voltage pulse is proportional to the energy deposited in the corresponding detector by a particle or a photon crossing the detector, and to the respective dose. By an 8-bit ADC these amplitudes are digitized and organized in a deposited 256 channels energy spectrum for every one of the detectors.

The gains of Liulin-MO preamplifiers CSA1 to CSA4 are a compromise between the conflicting goals of measuring gamma rays, electrons and high-energy protons (which have very low LET and hence require high gains) and covering the HZE spectrum (which requires low gains to measure highly ionizing particles such as iron). As a result of the compromise one of the detectors in every telescope measures and provides the energy deposition spectrum in the range 0.1–18 MeV (detectors D2 and D3), and the other in the range 0.4–190 MeV (detectors D1 and D4). The energy deposition spectra of D2 in the range 0.1–18 MeV and of D1 in the range 18.1–190 MeV are later summarized and used to obtain the energy deposition spectrum in the direction of D1–D2. The same procedure is used to obtain the energy deposition spectrum in the direction of D3–D4. In that way each dosemetric telescope provides data in the energy deposition range 0.1–190 MeV.

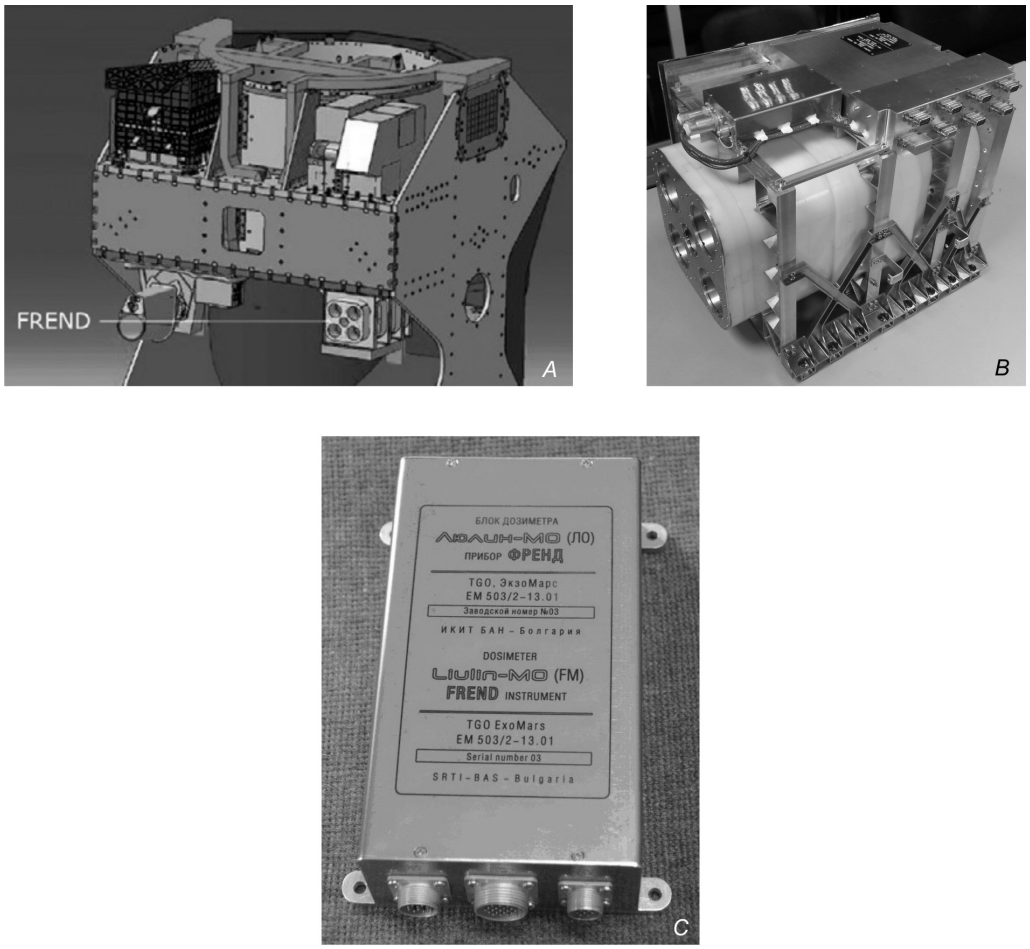

Fig. 3. *A*) FREND accommodation on the TGO (Credit: Thales Alenia Space – France `http://exploration.esa.int/mars/48523-trace-gas-orbiter-instruments/?fbodylongid=2217`); *B*) the FREND instrument with Liulin-MO mounted on it; *C*) external view of Liulin-MO

A coincidence technique for the associated with every dosemetric telescope electric signals is applied to obtain the linear energy transfer (LET). The energy deposition spectra measured in D1 and D2 detectors in coincidence mode are recorded separately and used to obtain the LET spectrum in the direction of D1–D2. That LET spectrum consists of low and high LET parts. The low LET part is obtained from the D2 coincidence spectrum in energy range 0.1–18 MeV and the high LET part is obtained from the D1 coincidence spectrum in energy range 18.1–190 MeV. Similarly the energy deposition spectra measured in the D3 and D4 detectors in coincidence mode are recorded separately and used to obtain the LET spectrum in the perpendicular D3–D4 direction. In addition the instrument measures the energy deposition spectrum in D3 in coincidence with D2, allowing

estimation of the dose rate and particle flux in the D3–D2 direction as well. In that way the output parameters of Liulin-MO are provided simultaneously for three directions.

The energy deposition is converted to energy lost per unit of path length (dE/dx) in silicon as:

$$dE_i/dx = EL_i/h_D, \tag{2}$$

where dE_i/dx (keV µm^{-1}) is the energy lost per unit of path length in silicon in channel i, EL_i (keV) is the energy deposition in channel i, h_D (µm) is the thickness of the corresponding detector.

A constant factor is applied to relate dE/dx in silicon to LET in water. Applying the same average value of the ratio dE/dx in silicon and LET in water of 1.6, with an associated uncertainty of ±15% for GCRs like for RAD instrument [23], LET for water $LET(\mathrm{H_2O})$ is then found by the relation:

$$LET(\mathrm{H_2O}) = \frac{dE/dx}{1.6}. \tag{3}$$

By definition the dose D (Gy) is the energy in Joule deposited in 1 kg of matter. The absorbed dose in a silicon detector D_{Si} (Gy) is calculated by dividing the summarized energy deposition in the spectrum in Joules to the mass of the detector in kilograms:

$$D_{\mathrm{Si}} = \sum_{i=1}^{256}(EL_i)/MD = \sum_{i=1}^{256}(n_i A_i/k)/MD = k1\sum_{i=1}^{256}(n_i i)/MD, \tag{4}$$

where EL_i is the energy deposition in channel i in Joule, MD is the mass of the detector in kg. The energy deposition in MeV is proportional to the voltage amplitude A_i of the pulses in channel i and respectively to the spectral channel number i: EL_i (MeV) = $n_i A_i$ (V)/k (V MeV^{-1}), where n_i is the number of pulses in channel i, k (V MeV^{-1}) is a coefficient dependent on the preamplifier's sensitivity. $k1$ (J) is a coefficient converting the spectral channel number to the energy deposited by a single particle or a photon.

The values $\sum_{i=1}^{256} n_i$ and $\sum_{i=1}^{256} n_i i$ proportional to the flux and to the dose are calculated for each detector from the corresponding energy deposition spectrum measured for a given time and provided in the Liulin-MO output data.

The parameters provided by Liulin-MO are: absorbed dose rate in the range 10^{-7}–0.1 Gy h^{-1}; particle flux in the range 0–10^4 particle cm^{-2} s^{-1}; energy deposition spectrum in the range 0.1–190 MeV; LET($\mathrm{H_2O}$) spectrum in the range 0.2–395 keV µm^{-1}. The above parameters are provided for three directions simultaneously. The dose rates and the fluxes are resolved every minute, while

the energy deposition spectra and the LET spectra are resolved every hour. The telemetry data rate is 250 kByte/day.

The dosemeter Liulin-ML for ExoMars 2018 will be similar to Liulin-MO dosemeter developed for ExoMars 2016 mission.

6. Liulin-MO calibration. The Liulin-MO dosemeter has been electronically calibrated using electrical test pulses through a small capacitor (1–2 pF) to inject a test charge into the input of each CSA. The amplitude A_i of the voltage pulses at the output of each CSA was measured and the corresponding spectral channel i was obtained. In that way the value of $k1$ in (4) that converts the spectral channel number to the deposited energy by a single particle or a photon was obtained for each of the Liulin-MO detectors.

Liulin-MO has been physically calibrated using standard γ-sources. Figure 4 presents the calibration diagram that shows the dependence of dose rate measurements in detector D3 (in relative units) on the dose rate of γ-sources used (dose rate is estimated at the centre of the parallelepiped formed by all four detectors). The linear approximation of that dependence is also shown. Those calibrations confirm the large dynamic ranges of the flux (up to 10^4 particle cm^{-2} s^{-1}) and the dose rate (10^{-7}–0.1 Gy h^{-1}) measurements that allow Liulin-MO to measure the fluxes and dose rates both of the relatively low-intensity GCR and the occasional high-intensity powerful SEP events. The instrument has also enough sensitivity to measure the natural radiation background on the Earth surface that is used to control the proper operation of its detectors during the pre-flight tests.

7. Conclusions. A new charged particle telescope Liulin-MO for measuring the radiation environment on board the ExoMars 2016 Trace Gas Orbiter satellite as a part of the Fine Resolution Epithermal Neutron Detector (FREND) has been

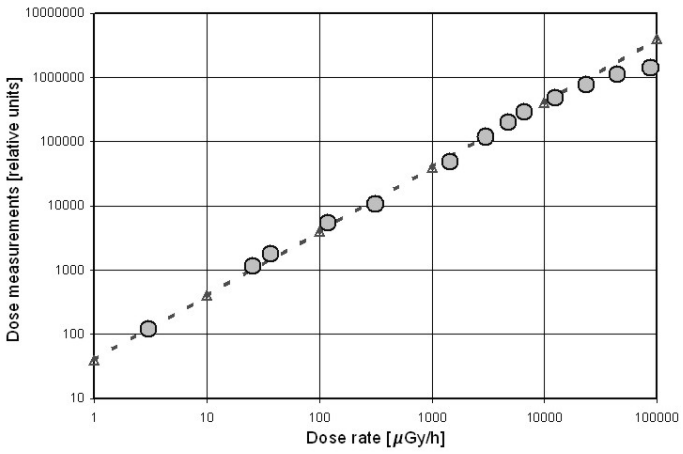

Fig. 4. Calibration curve of dose rate measurements in detector D3. The measured dose is marked with circles. Dashed line with triangles is the linear approximation

developed, calibrated and space flight qualified. The dynamic range of the LET spectrum (in H_2O) measured by Liulin-MO 0.2–395 keV μm^{-1} allows for the assessment of the contribution to the absorbed dose and to the dose equivalent of the electrons, protons and the high energy particles in the heavy ion cosmic component including highly ionizing particles such as iron, and the secondary charged particles and gamma radiation. The large dynamic ranges of the flux (up to 10^4 particle cm^{-2} s^{-1}) and the dose rate measurements 10^{-7}–0.1 Gy h^{-1} allows Liulin-MO to measure the fluxes and dose rates both of the relatively low-intensity GCR and the occasional high-intensity powerful SEP events. The launch of the ExoMars mission to Mars is planned for the beginning of 2016. A similar Liulin-ML experiment and instrument for investigation of the radiation environment on Mars as a part of the active detector of neutrons and gamma rays (ADRON) on the Russian surface platform is proposed for ExoMars 2018 mission. The charged particle telescopes will be used in combination with the neutron detectors of FREND and ADRON to study the radiation conditions from charged particles, neutrons and gamma rays during the cruise phase, in Mars orbit and on the surface of Mars.

REFERENCES

[1] Mewaldt R. A. (1996) http://www.srl.caltech.edu/personnel/dick/cos_encyc.html.

[2] Simpson J. A. (1983) In: NATO ASI Series C: Mathematical and Physical Sciences (ed. M. M. Shapiro), **107**, Dordrecht, Reidel.

[3] Benton E. R, E. V. Benton (2001) Nucl. Instrum. and Methods in Physics Research, B, **184** No 1–2, 255–294.

[4] Horneck G. (1994) Acta Astronautica, **32**, 749–755.

[5] Kim M.-H. Y. et al. (2011) Acta Astronaut. **68**, No 7–8, 747–759.

[6] Dachev Ts. P. et al. (2011) Adv. Space Res., **48**, No 5, 779–791, doi: 10.1016/j.asr.2011.05.009.

[7] Buchvarova M., P. I. Y. Velinov (2010) Adv. Space Res., **45**, No 8, 1026-1034.

[8] Gronoff G. et al. (2011) Astronomy and Astrophysics, **529**, No 5, A143–A146.

[9] Mishev A. et al. (2012) Atmos. Solar-Terr. Phys., **89**, 1–7.

[10] Mishev A., P. I. Y. Velinov (2014) Atmos. Solar-Terr. Phys., **120**, No 12, 111–120.

[11] Cucinotta F. A. et al. (2011) NASA Tech. Paper 2011-216155. NASA Scientific and Technical Information (STI) Program, Hampton, VA.

[12] Methodical instructions MU 2.6.1.44-03-2004 (2004) Limiting the exposure of astronauts during spaceflight near Earth. Moscow, Federal Office "Medbioextrem" (in Russian).

[13] Wilson J. W. et al. (1991) NASA TP-3146.

[14] Slaba T. C. et al. J. Comput. Phys., **229**, No 24, 9397–9417.

[15] Schwadron N. et al. (2010) Space Weather **8**, S00E04.

[16] McKenna-Lawlor S. et al. (2012) Planetary and Space Science, **63–64**, 123–132.
[17] Gronoff G. et al. (2015) Adv. Space Res., **55**, 1799–1805.
[18] Wilson J. W. et al. (1991) NASA Reference Publ. 1257, Ch. 11, 420.
[19] Letaw J. R., S. Clerwater (1986) SCC Report 86-02.
[20] Velinov P. I. Y., L. Mateev (1991) Compt. rend. Acad. bulg. Sci., **44**, No 1, 31–34.
[21] De Angelis et al. (2007) Nucl. Phys., **B166**, 184–202.
[22] McKenna-Lawlor S. et al. (2015) Acta Astronautica, **109**, 182–193.
[23] Zeitlin C. et al. (2013) Science, **340**, 1080–1084, doi: 10.1126/science.1235989.
[24] Hassler D. M et al. (2014) Science, **343**, 1244797-1-1244797-6, doi: 10.1126/science.1244797.
[25] Dachev T. P. et al. (2015) Life Sciences in Space Research, **4**, 92–114.
[26] International Commission on Radiological Protection (1991) ICRP Report No 60. Oxford, Pergamon Press.
[27] Semkova J. (2007) Compt. rend. Acad. bulg. Sci., **60**, No 9, 957–966.
[28] Semkova J. et al. (2008) Proc. Int. Conf. Fundamental Space Research, Sunny Beach, Bulgaria, 23–28 Sept. 2008, 351–354, ISBN 978-954-322-316-9.
[29] Semkova J. et al. (2009) Proc. Int. Conf. Fundamental Space Research, Suppl. Compt. rend. Acad. bulg. Sci., 215–218, ISBN 978-954-322-316-9.
[30] Semkova J. et al. (2010) Adv. Space Res., **45**, No 7, 858–865, doi: 10.1016/j.asr.2009.08.027.

Space Research and Technology Institute
Bulgarian Academy of Sciences
e-mail: jsemkova@stil.bas.bg

**Space Research Institute*
Russian Academy of Sciences
Moscow, Russia
e-mail: malakhov@iki.rssi.ru

***State Scientific Center of Russian Federation*
Institute of Biomedical Problems
Russian Academy of Sciences
Moscow, Russia
e-mail: v_benghin@mail.ru